JOURNAL OF
CELLULAR
PLASTICS

Original Article

Journal of Cellular Plastics
2014, Vol. 50(6) 551–562

DOI: 10.1177/0021955X14539778
cel.sagepub.com
SAGE

Impact of foaming on the broadband dielectric properties of multi-walled carbon nanotube/polystyrene composites

Mohammad Arjmand[1], Mehdi Mahmoodi[2], Simon Park[2] and Uttandaraman Sundararaj[1]

Abstract

This study investigated the impact of foaming on the broadband dielectric properties of multi-walled carbon nanotube/polystyrene (MWCNT/PS) nanocomposites. Different carbon nanotube concentrations were prepared by blending of a 20 wt.% MWCNT/PS masterbatch and pure PS using a twin-screw extruder. A chemical blowing agent was used to foam the nanocomposites in a micro injection molding machine. Compression molding was applied to fabricate unfoamed nanocomposites for comparison purposes. Comparing the dielectric properties of unfoamed and foamed nanocomposites showed that foaming increased the percolation threshold, reduced DC and AC conductivities, widened the insulator–conductor transition window, and reduced the dissipation factor of the MWCNT/PS composites. These were attributed to deteriorated conductive network and inferior dispersion and distribution of MWCNTs coming from the presence of foam cells in the nanocomposites. The obtained results propose foaming as a promising technique to improve the dielectric properties of MWCNT/polymer composites.

Keywords

Injection foam molding, polystyrene foams, chemical foaming/blowing agent, dielectric properties, carbon nanotube

[1]Department of Chemical and Petroleum Engineering, University of Calgary, Calgary, Canada
[2]Department of Mechanical and Manufacturing Engineering, University of Calgary, Calgary, Canada

Corresponding author:
Uttandaraman Sundararaj, Department of Chemical and Petroleum Engineering, University of Calgary, Calgary, Canada T2N 1N4.
Email: u.sundararaj@ucalgary.ca

Introduction

Desirable processability, low cost, light weight, and corrosion resistance of polymer matrices can be visualized as aiding factors to miniaturize and improve the world of embedded capacitors. However, pure polymers show poor dielectric permittivity for charge storage applications (e.g. $k < 3$), thus, increasing the dielectric permittivity of polymers used for charge-storage applications has been the subject of many studies.

Several strategies have been proposed to raise the dielectric permittivity of pure polymers,[1–4] among which adding conductive filler to polymer matrix is deemed to have a promising perspective. Different conductive fillers, such as carbon black, carbon nanotube (CNT) and nickel, gold and silver nanoparticles have been used to make composites for charge-storage purposes.[5–8] Among these, CNTs have been reported as revolutionary conductive fillers for charge-storage applications due to their large surface area and superior electrical properties.

High dielectric permittivity in CPCs is obtainable at filler loadings close to and above the percolation threshold. This is due to the formation of a large number of nanocapacitors structures, i.e. conductive filler as nanoelectrode and polymer matrix as nanodielectric.[4,9] Nonetheless, the insulator–conductor transition around the percolation threshold impedes using CPCs as charge storage materials above the percolation threshold. Thus, the major challenge in handling CPCs for charge storage applications is to control the insulator–conductor transition and dielectric loss around the percolation threshold.

Many studies have focused on deteriorating conductive network formation to control insulator–conductor transition, such as coating the surface of the conductive filler with a thin insulating layer,[10] using surface-oxidized metallic particles and nanowires,[11,12] aligning conductive filler,[13] and incorporating a secondary particle as insulating barrier.[14] Herein, we investigate injection foam molding as a potential technique to regulate conductive network formation. Foaming of nanocomposites is a well-established method and has been focus of many studies to manipulate the physical properties of nanocomposites, especially to decrease the percolation threshold.[15–19] Manipulating conductive network using injection foam molding is industrially more cost-effective and time-efficient than the other mentioned techniques since it does not need any further processing of conductive filler and can be employed as a mass production technique. Comparing the broadband dielectric properties of the foamed and unfoamed multi-walled carbon nanotube/polystyrene (MWCNT/PS) composites showed that foaming broadened the insulator–conductor transition window and reduced the dissipation factor.

Materials and experiments

A 20 wt.% MWCNT/PS masterbatch (Hyperion Catalysis International, Cambridge, MA) was diluted into concentrations of 0.1, 0.3, 0.5, 1.0, 2.0, 3.5, 5.0, and 10.0 wt.% of MWCNT in a PS matrix using a co-rotating twin-screw extruder. The nanotubes were vapor grown with an outer diameter of 10–15 nm

wrapped around a hollow 5 nm diameter core, ranging between 1 and 10 μm in length. According to the manufacturer, their density was approximately 1.75 g/cm^3. Polystyrene (Styron® 610) with a density of 1.06 g/cm^3 and a melt flow index of 10.0 g/10 min (200°C/5 kg) was kindly provided by Americas Styrenics LLC.

Before processing, all the materials were dried at 80°C for at least 4 h. Azodicarbonamide (Celogen AZ 130, Lion Copolymer, Baton Rouge, LA) was employed as the chemical blowing agent (CBA). The density of the CBA was about 0.60 g/cm^3 and the decomposition temperature and gas yield were about 190–220°C and 220 cm^3/g, respectively.

The foamed samples were fabricated using a micro injection molding machine (Boy 12 A) with a screw diameter of 18 m and a length to diameter (L/D) ratio of 20. A Celogen AZ concentration of 5 wt. % was evenly mixed with the nanocomposites in an electrical blender. The injection molding temperature was 215°C. The injection pressure and velocity were set at 100 bar and 240 mm/s, respectively; and, the mold temperature was set at 80°C to minimize unfoamed skin. The high injection velocity and mold temperature were fixed, so that the dispersed gas bubbles created the necessary expansion after injection, when the melt viscosity was still low enough for cell expansion.

The relative density of the foamed samples, defined as the density of the foamed composite divided by that of the unfoamed composite was measured between 0.55 and 0.65. Foamed samples with a relative density of about 0.6 were selected for the experiments. We assumed that the wt.% of the MWCNTs in the foamed composites was the same as the unfoamed composites, due to the negligible wt.% of the blown gas.

A rectangular cavity equipped with a trapezoidal runner and an edge gate was designed and fabricated for the foaming of the samples. The thickness of the cavity was 3 mm. Figure 1 shows a schematic of the mold employed in the injection molding process with the dimensions provided in Table 1. The mold was manufactured using a three-axis micro machining center (Kern Micro) using a tungsten carbide (WC) 700 μm taper-end mill tool with a taper angle of 2° and a spindle speed of 100,000 r/min.

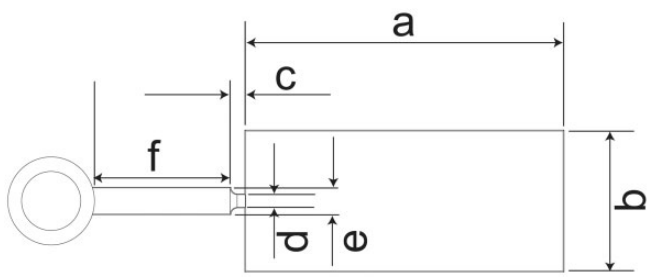

Figure 1. Schematic view of the designed mold.

Table 1. Dimensions of the designed mold.

Parameter	*a*	*b*	*c*, *d*	*e*	*f*
Value (mm)	22.86	10.16	1	2	10

A Carver compression molder (Carver Inc., Wabash, IN) was employed to fabricate the compression molded samples with the same dimensions as the injection molded samples. The compression molding process was carried out at 215°C for 10 min under 38 MPa pressure.

The morphology of the foamed nanocomposites was characterized employing scanning electron microscopy (SEM) and transmission electron microscopy (TEM) techniques. A high resolution Philips XL30 was used to obtain SEM images. All the samples were cryo-fractured prior to the SEM tests. TEM tests were performed using a Hitachi H-7650. The TEM analysis of the nanocomposites was carried out on ultramicrotomed sample sections using a Tecnai TF20 G2 FEG-TEM (FEI, Hillsboro, OR) at a 200 kV acceleration voltage with the standard single-tilt holder. The images were captured on a Gatan UltraScan 4000 CCD (Gatan, Pleasanton, CA) at 2048 x 2048 pixels. The samples were ultramicrotomed to sections of ~70 nm at room temperature using a Leica EM UC6.

DC electrical conductivity testing was conducted on the samples in the thickness direction using two different setups. A Keithley 6517A electrometer connected to a Keithley test fixture (Keithley instruments, USA) was used for the samples with conductivities lower than 10^{-2} S m^{-1}. For the samples with electrical conductivities higher than 10^{-2} S m^{-1}, a Loresta GP resistivity meter (MCP-T610 model, Mitsubishi Chemical Co., Japan) connected to an ESP four-pin probe was used, according to the ASTM 257-75. The four-pin probe eliminated the effect of contact resistance. The applied voltage was 10 V for all the DC conductivity tests. An impedance gain-phase analyzer (Solartron SI 1260) was used to measure the dielectric properties of the nanocomposites in the frequency range of 10^1–10^6 Hz. Silver paste was used to paint the electrodes on the samples prior to the measurements.

Results and discussion

Morphological characterization

Figure 2a shows a SEM micrograph from a typical skin-core structure of the foamed nanocomposites (5.0 wt.% MWCNT loading). Due to large temperature differences between the hot polymeric melt and the cold walls of the injection mold, an unfoamed skin solidifies on the foamed core. Figure 2b shows a SEM micrograph taken from the core of the nanocomposite. As can be seen in the SEM micrograph, the cell sizes ranged approximately from 1 to 150 μm. At a clearly higher resolution image from the foamed nanocomposite, MWCNTs can be observed as bright spots in the PS matrix (Figure 2c). Due to difference in the

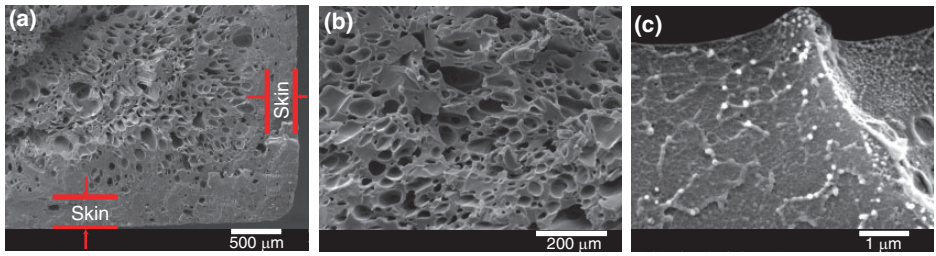

Figure 2. SEM images of the foamed MWCNT/PS nanocomposites: (a) a low-magnification SEM image showing the skin-core structure of a 5.0 wt.% MWCNT foamed composite, (b) a low-magnification SEM image of the core from a 5.0 wt.% nanocomposite, and (c) a high-magnification SEM image from a 5.0 wt.% nanocomposite.

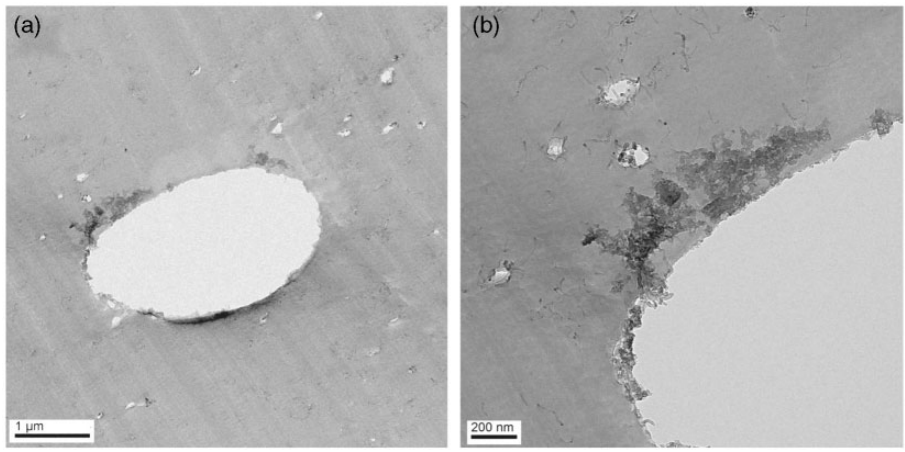

Figure 3. TEM images of the foamed MWCNT/PS nanocomposites: (a) low-magnification and (b) high magnification.

charge transfer capability of MWCNTs and polymer matrix, secondary electrons are intensified at the location of MWCNTs. This leads to contrast between MWCNTs and polymer matrix in SEM imaging.[20]

Figure 3 shows the TEM images of the injection foamed molded samples at low and high magnifications. One can assume that, during the cell growth step of the chemical injection foam molding method, the formation of conductive networks was deteriorated and agglomerates of MWCNTs were formed around the foam cells. In fact, in this method, a portion of the cavity was first filled with the polymeric melt mixed with the blowing agent; and, the rest of cavity was then quickly filled by cell expansion induced by the pressure drop. This led to deterioration of conductive networks and formation of MWCNT agglomerates around the foam cells.

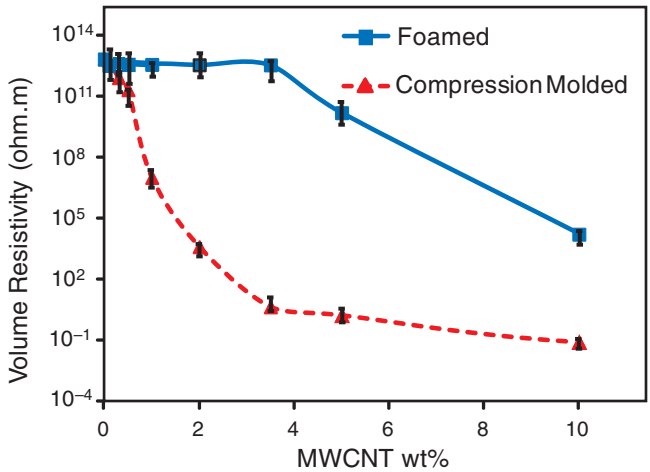

Figure 4. DC electrical resistivity of the foamed and unfoamed MWCNT/PS molded nanocomposites.

DC and AC electrical conductivity

The new generation of microelectronics demands polymer-based capacitors with high dielectric permittivities and low dielectric losses. According to the percolation theory, CPCs appropriate for charge storage applications can be obtained at filler loadings very close to the percolation threshold.[5,21] Therefore, studying the percolation behavior of the foamed conductive filler/polymer nanocomposites is a necessity prior to investigating their dielectric performance.[22,23]

The DC electrical resistivity versus MWCNT loading is shown in Figure 4 for both the compression molded and injection foamed molded nanocomposites. Employing the percolation theory, the compression molded samples showed percolation threshold equal to 0.7 wt.%, however it was interestingly observed that the injection foamed molded samples presented insulative behavior even up to 3.5 wt.%. The logarithms of the volume resistivity for the compression molded samples at 0.5, 1.0, and 2.0 wt.% MWCNT loadings were 11.28, 6.98, and 3.57, respectively, showing an insulator–conductor transition in the concentration window of 0.5–2.0 wt.%. The logarithms of the volume resistivity of the foamed nanocomposites at 3.5, 5.0, and 10.0 wt.% were 12.51, 10.16, and 4.19, respectively, indicating an insulator–conductor transition window of 3.5–10.0 wt.%.

The broad insulator–conductor transition window of the foamed nanocomposites can be attributed to their unique structure. In fact, foam cells deteriorate conductive networks and avoid a sharp insulator–conductor transition. Broad insulator–conductor transition window reduces the risk of manipulating CPCs for charge storage applications around the percolation threshold.[13,14] Thus, it can be claimed that foaming can be used as an efficient technique to improve the safety of manipulating CPCs for charge storage applications.

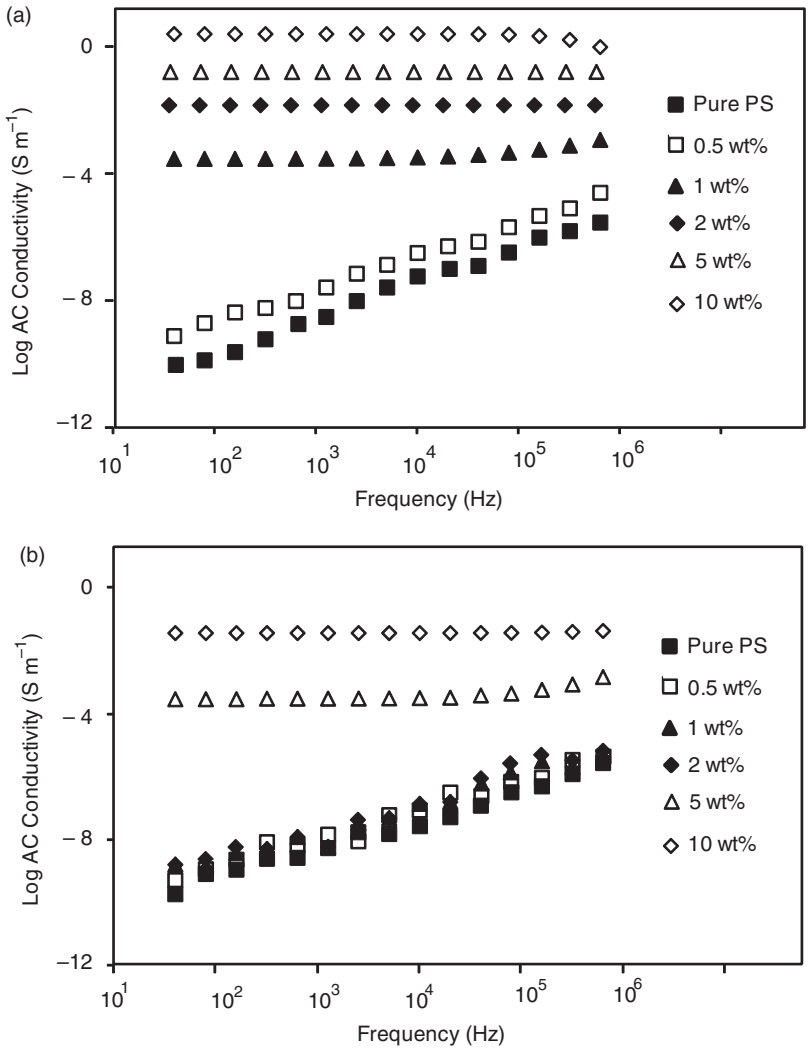

Figure 5. AC conductivity versus frequency for (a) compression molded and (b) foamed MWCNT/PS nanocomposites.

Figure 5 presents the logarithm of AC conductivity (σ_{AC}) versus frequency at various MWCNT loadings. Generally, AC conductivity is defined as following[24,25]:

$$\sigma_{AC} = \varepsilon'' \omega \varepsilon_0 + i(\varepsilon' \omega \varepsilon_0) \tag{1}$$

where σ_{AC}: AC conductivity, ε': dielectric permittivity, ε'': dielectric loss, ω: angular frequency, and ε_0: permittivity of free space. This equation shows that the real part of AC conductivity is proportional to dielectric loss and occurs due to flow of

charges through the dielectric material (leakage current). The imaginary part of AC conductivity occurs to compensate for the charges which are polarized inside the dielectric material. In fact, the current due to imaginary conductivity does not pass through the dielectric but moves in the circuit to compensate for the charges which are stored on the surface of capacitor.

It is well known that AC conductivity is a strong function of frequency in the insulative region, however it is almost constant in the conductive region.[9] As a matter of fact, at low conductive filler contents because of large insulative gaps between conductive fillers, the DC conductivity (low-frequency AC conductivity) is very low. However, with frequency increase, the role of capacitive currents highlighted, since high-frequency voltage facilitated frequent development of capacitive currents in a time frame. This causes drastic change in conductivity as a function of frequency in the insulative region.

As clearly shown in Figure 5a, the σ_{AC} of the pure PS and the compression molded 0.5 wt.% MWCNT loaded composite showed an ascending trend with frequency. In comparison, the σ_{DC} of the compression molded 0.5 wt.% MWCNT loaded nanocomposite showed that the molded sample was insulative at this MWCNT loading. With further increases in MWCNT loading, the σ_{AC} was almost independent of the frequency signifying a conductive region. For the foamed specimens, the σ_{AC} was frequency dependent for 0.5, 1.0, and 2.0 wt.% MWCNT/PS nanocomposites and it became frequency independent at 5.0 and 10.0 wt.%. These results are in agreement with the DC conductivity data and confirm the impact of foaming on deteriorating conductive network formation and increasing the percolation threshold.

Dielectric spectroscopy

The dissipation factor (or loss tangent, known as tan δ) is the ratio of the dielectric loss to the dielectric permittivity. Dielectric permittivity represents the charges stored on the surface of dielectric material and originates from charge polarization within dielectric. Dielectric loss shows how dissipative a dielectric is under an alternating field, and should be kept low for charge storage applications. Thus, dissipation factor is a measure of the energy loss to the energy stored in a periodic field[12,25]; and its low amount is highly desirable for charge storage applications.

Figure 6 shows the dissipation factor of the molded nanocomposites over the measured frequency. Considering the percolation thresholds of the molded samples, we claim that the dissipation factor was a weak function of frequency for the insulative nanocomposites, but it showed a strong descending trend for the conductive nanocomposites. Second, the injection foamed molded nanocomposites showed a much lower dissipation factor than the compression molded nanocomposites. For example, for 1.0 and 2.0 wt.% MWCNT/PS nanocomposites at 80 Hz, the dissipation factor of the compression molded samples were 1.97×10^2, 1.31×10^5, respectively, whereas it was interestingly observed that the foamed

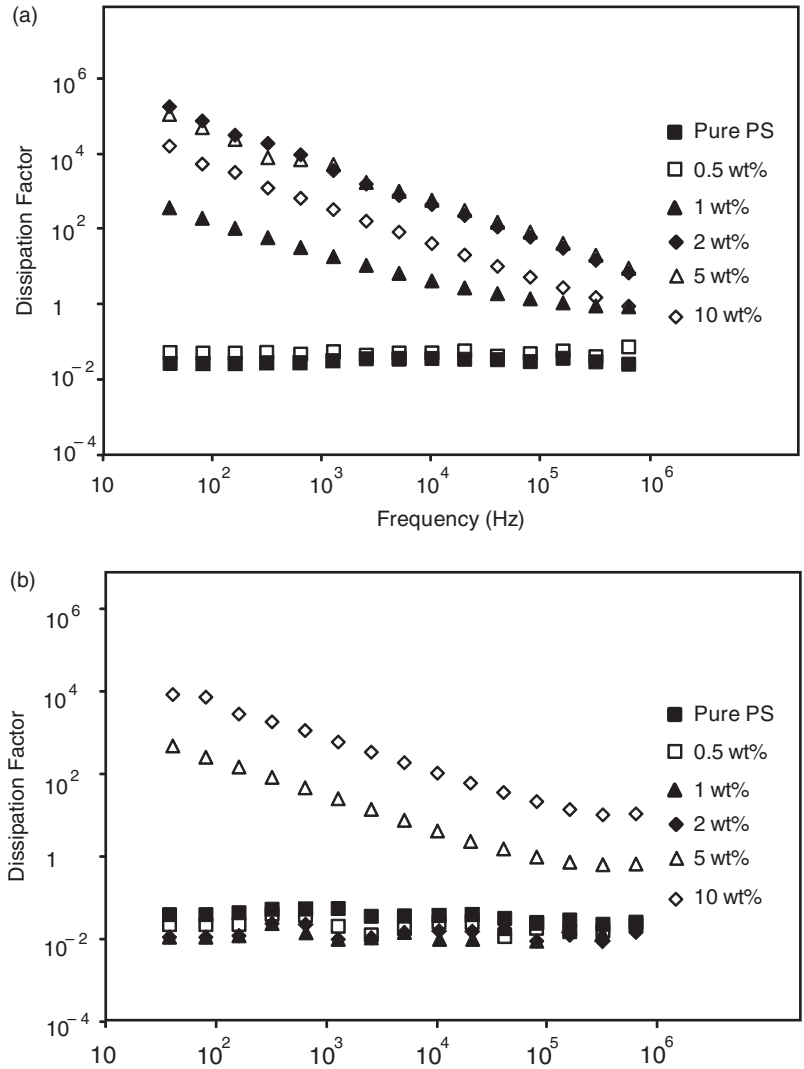

Figure 6. Dissipation factor versus frequency for (a) compression molded and (b) injection foamed molded MWCNT/PS nanocomposites.

molded samples presented dissipation factors significantly lower and equal to 1.14×10^{-2} and 1.21×10^{-2}, respectively.

The lower dissipation factor of the injection foamed molded nanocomposites can be attributed to their lower dielectric loss. In fact, in the injection foamed molded samples due to inferior dispersion and distribution of MWCNTs, a poorer conductive network was formed. At a poorer conductive network

formation, the electrons have less mean free path to move in each half cycle of alternating field and thus less electrical energy is dissipated.[26]

In conclusion, the obtained results showed that chemical injection foam molding of MWCNT/polymer nanocomposites can be considered as a promising strategy to reduce dissipation factor and broaden insulator–conductor region. The positive impact of foaming in improving the dielectric properties of MWCNT-filled nanocomposites can be considered as a significant industrial achievement, since injection foam molding can be employed as a mass-production technique for polymer nanocomposites.

Conclusion

This study investigated the impact of foaming on the broadband dielectric properties of MWCNT/PS nanocomposites. Accordingly, the dielectric properties of compression molded samples were compared with those of injection foamed molded samples. Morphological characterization showed that during the cell growth step of the injection foam molding method, the formation of conductive networks was deteriorated and agglomerates of MWCNTs were formed around the foam cells. It was also observed that foaming increased the percolation threshold, broadened the insulator–conductor transition window, and reduced the dissipation factor of the MWCNT/PS nanocomposites. These were attributed to inferior conductive network formation and poorer dispersion and distribution of MWCNTs in the PS matrix arising from the presence of foam cells in the composites. The positive impact of foaming on improving the dielectric properties can reduce the risk of manipulating CPCs around the percolation threshold for charge storage applications.

Acknowledgment

The authors would like to thank Dr Tieqi Li and Ms. Jeri-Lynn Bellamy in Nova Chemicals®, Calgary, AB, Canada for the polymer extrusion/blending. We would like to gratefully acknowledge Dr Shamiul Islam and Dr Josephine M Hill for assistance with the dielectric properties measurements. We are grateful to Americas Styrenics LLC, for providing the neat polystyrene.

Conflict of interest

The authors declared no potential conflicts of interest with respect to the research, authorship, and/or publication of this article.

Funding

This study was financially supported by the Natural Sciences and Engineering Research Council (NSERC) of Canada and Alberta Innovates Technology Futures (AITF).

References

1. Shen Y, Lin Y, Li M, et al. High dielectric performance of polymer composite films induced by a percolating interparticle barrier layer. *Adv Mater* 2007; 19: 1418–1422.

2. Zhang QM, Li H, Poh M, et al. An all-organic composite actuator material with a high dielectric constant. *Nature* 2002; 419: 284–287.
3. Lei YJ, Zhao R, Zhan YQ, et al. Generation of multiwalled carbon nanotubes from iron-phthalocyanine polymer and their novel dielectric properties. *Chem Phys Lett* 2010; 496: 139–142.
4. Yao SH, Yuan JK, Dang ZM, et al. High dielectric performance of three-component nanocomposites induced by a synergistic effect. *Mater Lett* 2010; 64: 2682–2684.
5. Qi L, Lee BI, Chen SH, et al. High-dielectric-constant silver–epoxy composites as embedded dielectrics. *Adv Mater* 2005; 17: 1777–1781.
6. Wang L and Dang ZM. Carbon nanotube polymer composite with high dielectric constant at low percolation threshold. *Appl Phys Lett* 2005; 87: 042903.
7. Xu JW and Wong CP. Dielectric behavior of ultrahigh-k carbon black composites for embedded capacitor applications. In: *Proceedings of ECTC conference*, Lake Buena Vista, 2005, pp.1864–1869.
8. Xu JW, Wong M and Wong CP. Super high dielectric constant carbon black-filled polymer composites as integral capacitor dielectrics. In: *Proceedings of ECTC conference*, Las Vegas, 2004, pp.536–541.
9. Jiang MJ, Dang ZM, Bozlar M, et al. Broad-frequency dielectric behaviors in multiwalled carbon nanotube/rubber nanocomposites. *J Appl Phys* 2009; 106: 84902–84906.
10. Yuan ZM, Yao SH, Dang ZM, et al. Giant dielectric permittivity nanocomposites: realizing true potential of pristine carbon nanotubes in polyvinylidene fluoride matrix through an enhanced interfacial interaction. *J Phys Chem C* 2011; 115: 5515–5521.
11. Lu J, Moon KS, Xu J, et al. Synthesis and dielectric properties of novel high-K polymer composites containing in-situ formed silver nanoparticles for embedded capacitor applications. *J Mater Chem* 2006; 16: 2543–2548.
12. Silva A, Arjmand M, Sundararaj U, et al. Novel composites of copper nanowire/PVDF with superior dielectric properties. *Polymer* 2013; 55: 226–234.
13. Arjmand M, Mahmoodi M, Park S, et al. An innovative method to reduce the energy loss of conductive filler/polymer composites for charge storage applications. *Compos Sci Technol* 2013; 78: 24–29.
14. Yao S-H, Dang Z-M, Jiang M-J, et al. $BaTiO_3$-carbon nanotube/polyvinylidene fluoride three-phase composites with high dielectric constant and low dielectric loss. *Appl Phys Lett* 2008; 93: 182905.
15. Wang C, Ying S and Xiao Z. Preparation of short carbon fiber/polypropylene fine-celled foams in supercritical CO_2. *J Cell Plast* 2013; 49: 65–82.
16. Antunes M, Gedler G and Velasco JI. Multifunctional nanocomposite foams based on polypropylene with carbon nanofillers. *J Cell Plast* 2013; 49: 259–279.
17. Yen Y-C, Lee T, Chiu D, et al. Polystyrene foams with inter-connected carbon particulate network. *J Cell Plast*. Epub ahead of print 2014. DOI: 10.1177/0021955X14527102.
18. Tran M-P, Detrembleur C, Alexandre M, et al. The influence of foam morphology of multi-walled carbon nanotubes/poly(methyl methacrylate) nanocomposites on electrical conductivity. *Polymer* 2013; 54: 3261–3270.
19. Ameli A, Jung PU and Park CB. Through-plane electrical conductivity of injection-molded polypropylene/carbon fiber composite foams. *Compos Sci Technol* 2013; 76: 37–44.

20. Loos J, Alexeev A, Grossiord N, et al. Visualization of single-wall carbon nanotube (SWNT) networks in conductive polystyrene nanocomposites by charge contrast imaging. *Ultramicroscopy* 2005; 104: 160–167.
21. Dang ZM, Yao SH, Yuan JK, et al. Tailored dielectric properties based on microstructure change in BaTiO3-carbon nanotube/polyvinylidene fluoride three-phase nanocomposites. *J Phys Chem C* 2010; 114: 13204–13209.
22. Ameli A, Nofar M, Park CB, et al. Polypropylene/carbon nanotube nano/microcellular structures with high dielectric permittivity, low dielectric loss, and low percolation threshold. *Carbon* 2014; 71: 206–217.
23. Ameli A, Jung PU and Park CB. Electrical properties and EMI shielding effectiveness of polypropylene/carbon fiber composite foams. *Carbon* 2013; 60: 379–391.
24. Grimes CA, Mungle C, Kouzoudis D, et al. The 500 MHz to 5.50 GHz complex permittivity spectra of single-wall carbon nanotube-loaded polymer composites. *Chem Phys Lett* 2000; 319: 460–464.
25. Arjmand M and Sundararaj U. Broadband dielectric properties of multi-walled carbon nanotube/polystyrene composites. *Polym Eng Sci*. Epub ahead of print 2014. DOI: 10.1002/pen.23881.
26. Arjmand M, Apperley T, Okoniewski M, et al. Comparative study of electromagnetic interference shielding properties of injection molded versus compression molded multi-walled carbon nanotube/polystyrene composites. *Carbon* 2012; 50: 5126–5134.